Information Horizons: AMERICAN Journal of Library And Information Science Innovation
Volume 4, Issue 03, 2026 ISSN (E): 2993-2777

SiO_2/Polyazomethine/Polyaniline Hybrid Nanocomposites: Synthesis and Characterization

Alaa Siawnn ALmyre *[1], Samia Mezhr Merdas [2]
[1,2]Department of Chemistry, College of Science, University of Thi-Qar, Iraq
**Corresponding Author E-mail: alaa.wadi@utq.edu.iq*
E-mail: samia.m_mschem@sci.utq.edu.iq

Abstract. *This investigation aims to standardize and characterize a novel nanopolymer composite of SiO_2/PAM/PAn The polymer composite is prepared via intermediate polymerization through condensation and is enhanced using silicon nanoparticles to increase its surface area and adsorption capacity. The material is characterized by Fourier transform infrared spectroscopy (FTIR) to identify functional groups, ray diffraction (DRX) to explore its structure, and barrier electron microscopy (MEB) to analyze its surface and porosity. Additionally, thermogravimetric analysis (ATG) and transmission electron microscopy (MET) are performed. Gel permeability chromatography (GPC) is also conducted, enabling the calculation of molecular and digital color and polymer stability.*

Keywords: *Nano copolymer, SiO2 nanocomposite, Polyaniline Polyazomethine.*

Introduction

The field of nanomaterials has garnered increasing attention in recent years due to the unique physical and chemical properties of these materials, which differ significantly from their macroscopic counterparts[1]. This is attributed to their small size and high surface-to-volume ratio[1]. Among these materials, silica nanoparticles (SiO_2) have received considerable attention due to their chemical stability, ease of preparation, and high potential for surface modification, making them ideal substrates for the fabrication of nanocomposites[2] .On the other hand, conductive polymers such as polyaniline (PANI) are promising materials for electronic and electrochemical applications, thanks to their excellent electrical properties, ease of preparation, and low cost[3]. Polyazomethine polymers, meanwhile, are characterized by the presence of C=N bonds, which confer thermal stability and distinctive optical and electrical properties, making them suitable for use in diverse fields such as sensing and photonics[4]. Combining silica nanoparticles with azomethine and polyaniline polymers to form a hybrid nanocomposite is an effective strategy for enhancing the properties of the final material[2, 3]. SiO_2 contributes to structural stability and increased specific surface area, while the polymers provide functional properties such as electrical conductivity and interaction with various molecules[2, 3]. This synergy between the components leads to the production of materials with performance superior to that of each component individually[5] .Therefore, this research aims to prepare a hybrid nanocomposite composed of silica nanoparticles, azomethine, and polyaniline polymers, and to study its structural and morphological properties using various diagnostic techniques. The goal is to evaluate its efficiency and potential for future applications in fields such as adsorption, sensing, and environmental science[4, 6], Despite significant advances in nanocomposite preparation, most previous studies have focused on binary systems combining silica nanoparticles with a conductive polymer such as polyaniline, or on the study of azomethine polymers separately[6]. However, the integration of these three components into a single hybrid nanocomposite has not received sufficient attention, particularly regarding the understanding of the synergistic effects of each component's structural, electrical, and morphological properties. Furthermore, the impact of azomethine (–C=N–) bonds with polyaniline on the surface of SiO_2 nanocomposites to enhance the final material's performance remains under-explored in the scientific literature[4]. Therefore, a systematic study is needed to highlight the preparation of this type of tertiary composite and accurately characterize its properties in order to address this knowledge gap and assess the potential for developing more efficient materials for diverse applications.[4].

Materials and Methods

Raw Materials

Terephthalaldehyde,1,5-Diaminonaphthalene (SANTA CRUZ USA). Hydrochloric acid (BDH), Aluminum hydroxide (Merck),Potassium Persulfate (CDH). Sodium Hydroxide(CDH) , Dimethylformamide (CDH) , Aniline (CDH) .

Preparation of SiO_2 Nanoparticless

Silica oxide was produced using an environmentally friendly method from rice husks[7]. The process began by thoroughly washing the husks several times under running water, followed by rinsing with deionized water. The husks were then dried at 70°C for 24 hours. The dried husks were then heat-treated in a closed oven at 900°C for 7 hours to remove carbon. Next, 5 grams of the ground husks were dissolved in 500 mL of 0.5 M sodium hydroxide solution, and the mixture was heated with continuous stirring for 4 hours[8]. The resulting mixture was washed and filtered with deionized water, and the pH of the solution was adjusted to 7 using hydrochloric acid. The resulting silica gel was left to stand for 24 hours, then centrifuged, and finally dried in an electric oven at 70°C for 6 hours[9].

$$Na_2SiO_3 + 2HCl \rightarrow Si\,O_2 + H_2O + 2NaCl \ \ldots\ldots\ldots\ldots\ldots\ (1)$$

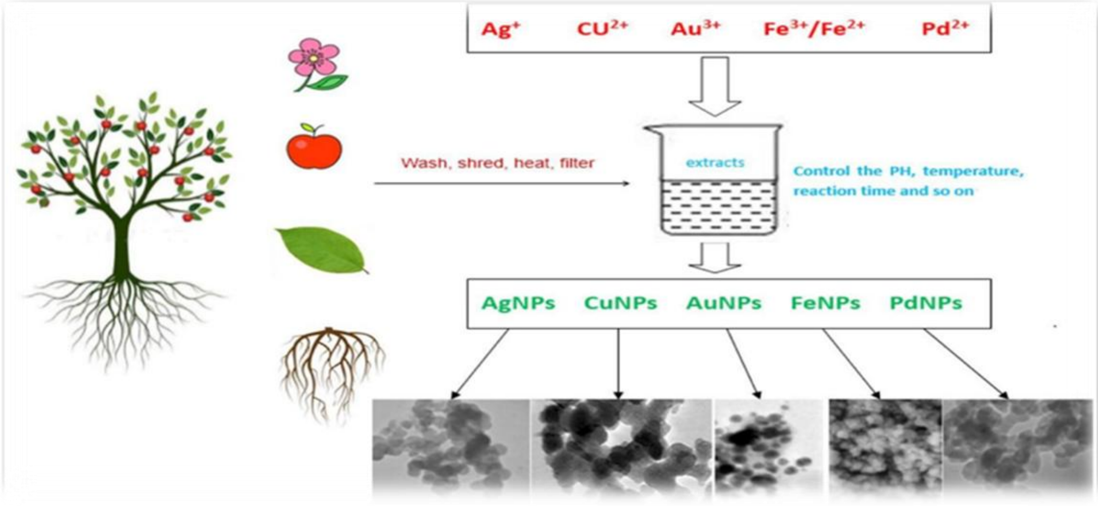

Figure 1. Green synthesis

Preparation of polyazomethene(PAM)

The polymer was synthesized via a condensation polymerization process, where the two compounds reacted in a 1:1 ratio[10]. A precise amount of 0.1341 g of terephthalide carboxaldehyde was dissolved in 10 mL of dimethylformamide (DMF). After complete dissolution, the solution was transferred to a 100 mL three-necked flask, where magnetic stirring was used to ensure homogeneous mixing of the compound and solvent. The temperature was maintained at 90 °C, and two drops of glacial acid were added to accelerate the reaction. Subsequently, 0.1582 g of 1,5-naphthylenediamine was dissolved in another 10 mL of DMF and gradually added to the flask in batches to achieve optimal results and ensure complete dissolution of both the compound and solvent. The reaction was allowed to stand for 12–18 hours, during which time an increase in the viscosity of the solution indicated polymer formation. After the reaction time was complete, the solution was allowed to cool to room temperature, then poured into 400 mL of deionized water to precipitate the polymer[11]. The precipitate was filtered and washed with deionized water and a small amount of ethanol to remove any remaining monomers and solvent. Finally, the product was dried in a vacuum oven at 50–60 °C for 12 hours[12].

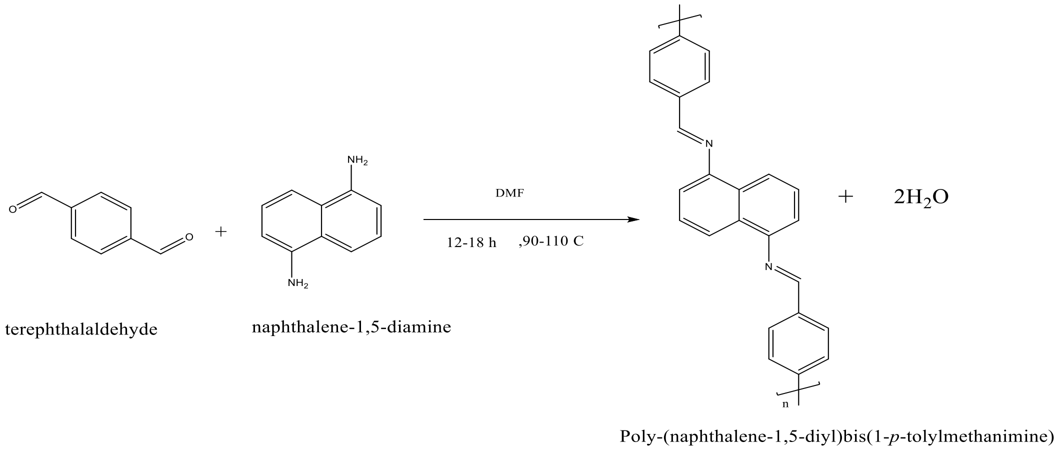

Equation 2: Preparation of polyazomethenyl(PAM)

Preparation of polyaniline (Poly An)

Dissolve 20 mL of aniline in 40 mL of 1 M hydrochloric acid in a 200 mL container of precipitate and keep refrigerated at 5°C. This mixture is called Mezcla 1. Next, dissolve 20 g of sodium sulfate in 160 mL of 1 M hydrochloric acid, which is called Mezcla 2. Gently and carefully add Mezcla 2 to Mezcla 1, removing it continuously over two hours. Then, allow the mixture to stand at ambient temperature for 24 hours. Once finished, filter the mixture and enjoy the resulting product with water, ethanol, and acetone. Finally, continue heating the mixture to 80°C for three hours[13].

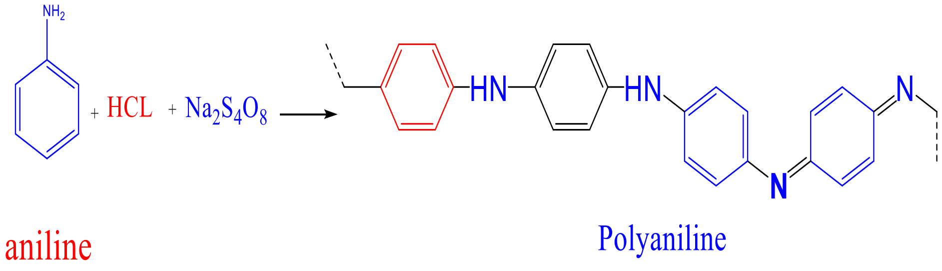

Equation 3: Preparation of polyaniline (Poly An)

Preparation of polymeric nanocomposites(SiO_2/PAM)

The preparation of the nanopolymer composite began with the precise measurement of 0.5 g of nanosilica, which was dissolved in 10 mL of dimethylformamide (DMF) solvent. This mixture was stirred for 15 minutes to ensure homogeneity. The nanosilica was then ultrasonically treated for 30 minutes to ensure uniform dispersion in the solvent. Next, 0.1341 g of terephthalide carboxaldehyde was placed in a three-necked flask, and the pre-dispersed nanosilica was gradually added while continuously stirring and heating. During this process, a few drops of glacial acid were added to the mixture. Stirring continued for another 30 minutes. Finally, 0.15812 g of 1,5-naphthylenediamine was dissolved in 10 mL of DMF and added to the flask in batches. During the reaction, the temperature, consistency, and color changes of the mixture were carefully monitored, allowing the reaction to continue for 18 hours to ensure the polymer was formed as planned, according to the specified reaction equation[14].

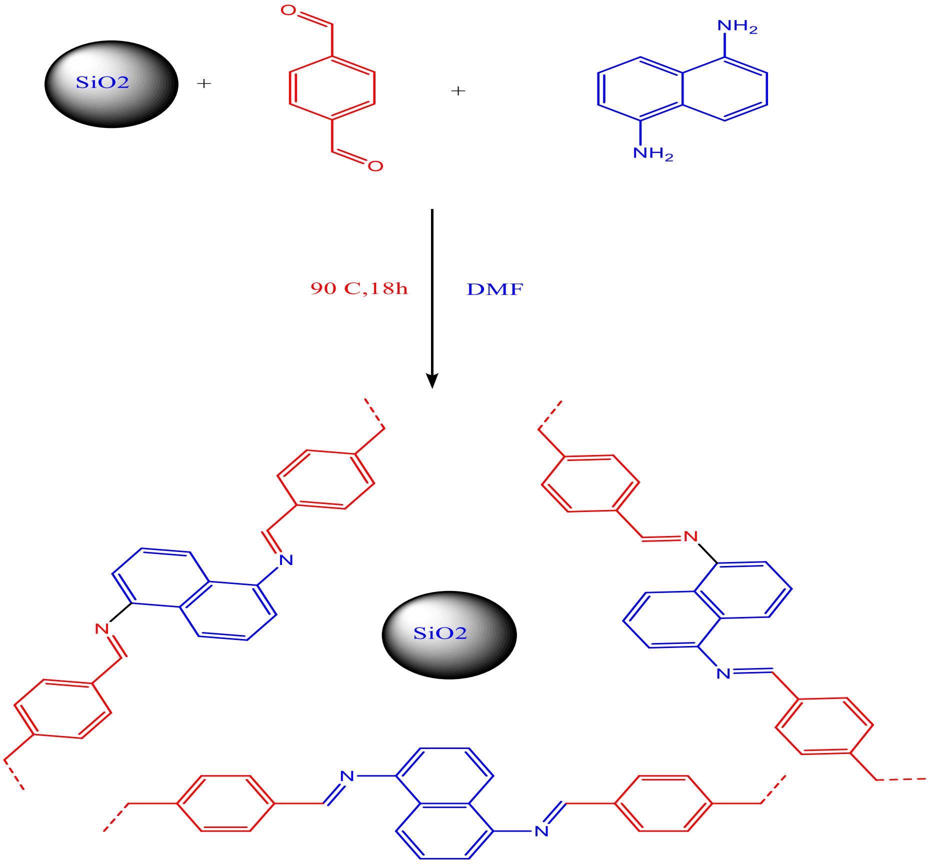

Equation4: Preparation of polymeric nanocomposites(SiO2/PAM)

Preparation of nanocopolymer (SiO_2/PAM/PAn)

Weigh out 0.5 grams of the pre-prepared nanocomposite SiO2/PAM1 and disperse it in 10 milliliters of deionized water. This is done by placing it in an ultrasonic device at a temperature of 25 degrees Celsius for half an hour to ensure the nanopolymer is thoroughly mixed with the deionized water. Next, transfer the mixture into a 200-milliliter beaker. In a separate step, dissolve 20 milliliters of aniline in 40 milliliters of 1 M hydrochloric acid, and keep this mixture in a beaker on ice at a temperature of 0 degrees Celsius; this will be referred to as mixture one. Simultaneously, dissolve 12 grams of sodium persulfate in 160 milliliters of 1 M hydrochloric acid at 5 degrees Celsius, which will serve as mixture two. Carefully and slowly add mixture two to mixture one, allowing the combined mixture to stir for two hours. Afterward, let it sit at room temperature for 24 hours. Once the time has elapsed, filter the mixture and wash the resulting product with deionized water, ethanol, and acetone. Finally, dry the product in an oven at 80 degrees Celsius for three hours[15, 16].

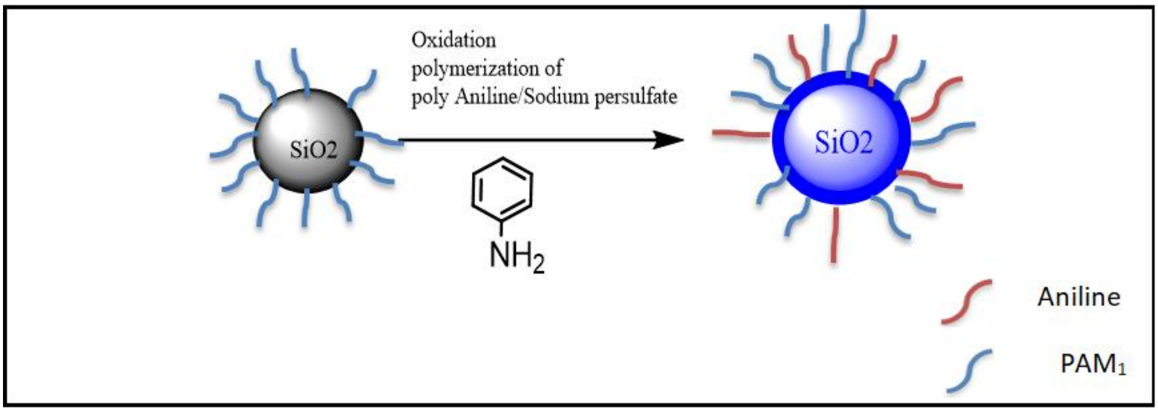

Figure 2. Preparation of nanocopolymer (SiO2/PAM/PAn)

Results and Discussion

FT-IR Spectra of SiO_2 Nanoparticles

Figure 3 shows the infrared spectrum of the nanomaterial, which exhibits a strong absorption band at 3630.03 cm^{-1}[17], attributed to the presence of the Si-OH group on the silica surface. Additionally, an absorption band at 1043.49 cm^{-1} is associated with the asymmetric Si-O-Si group[17]. Another absorption band appears at 948.98 cm^{-1}, also associated with the Si-OH group, while a band at 470.63 cm^{-1} is attributed to the vibration of the Si-O bond[18].

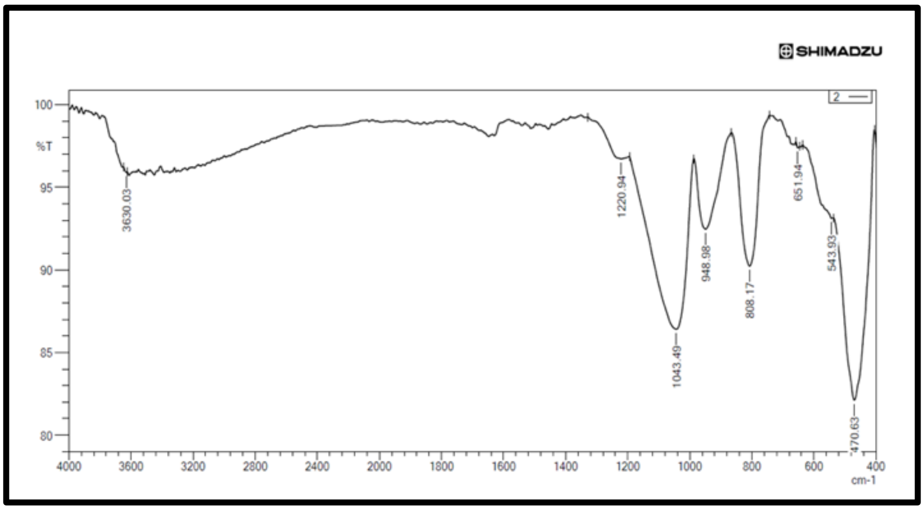

Figure 3. FT-IR Spectra of SiO2 Nanoparticles

FT-IR Spectra of SiO_2 /PAM/PAn

Figure 4 shows the infrared spectrum of the polymer (SiO2/PAM/An). This polymer exhibits a broad absorption band at 3358.46 cm^{-1}, attributed to the presence of (N-H) groups. In addition, there is an absorption band at 3232.40 cm^{-1} associated with (Si-OH) groups, and another at 2915.23 cm^{-1} associated with azomethine (C-H) groups. The spectrum also reveals absorption bands at 1644.13 cm^{-1}, corresponding to the stretching vibration of the azomethine (C=N) bond, as well as a band at 1554.91 cm^{-1} resulting from the stretching vibration of the aromatic (C=C) bond. In addition, an absorption band at 1400 cm^{-1} is associated with the aromatic bond (C=C), and a band at 1070.74 cm^{-1} is attributed to the bond (Si-O-Si)[19, 20].

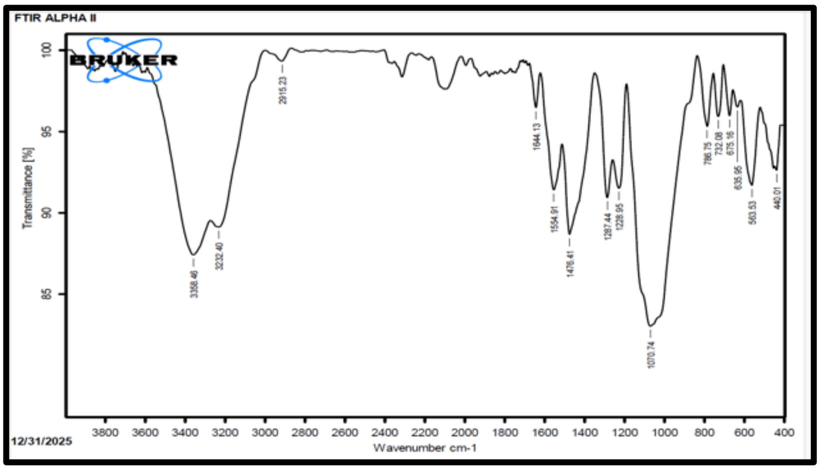

Figure 4. FT-IR Spectra of SiO2 /PAM/Pan

The TEM Photographs of SiO_2 Nanoparticles

Transmission electron microscopy (TEM) analysis shows that the SiO_2 nanoparticles are spherical or spherical, with a noticeable contrast between the particles and the background due to density differences. The size of these particles typically falls within the nanometer range (10–100 nm), indicating successful preparation. Agglomeration was also observed due to the high surface energy of the nanoparticles. Figure 3–5 shows a reasonable particle distribution with a slight variation in size. Furthermore, the absence of distinct crystalline patterns suggests that the material is amorphous[21]

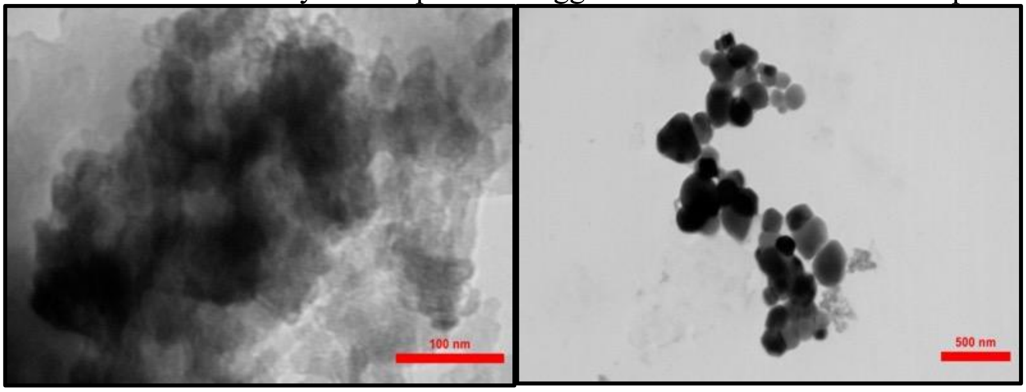

Figure 5. TEM of SiO_2 Nanoparticles

X-ray diffraction for nanoscale SIO_2 diagnosis

This technique provides information about the crystalline structure, chemical composition, and physical properties of materials and thin films of crystalline materials. The crystallinity index (CI) can be calculated from the X-ray diffraction spectrum using the following equation:

CI% =[(Im-Iam)/Im]*100……………..(1)

Where Im represents the maximum intensity of the crystalline segment at (2θ), and Iam represents the diffraction intensity of the amorphous segment at (2θ). The crystallinity index (CI) provides information about the crystalline state, as broad diffraction peaks appear in the nanomaterial's X-ray diffraction spectrum, and a broad band is observed at (22° = 2θ), indicating reflection at this angle for the nanomaterial[17].

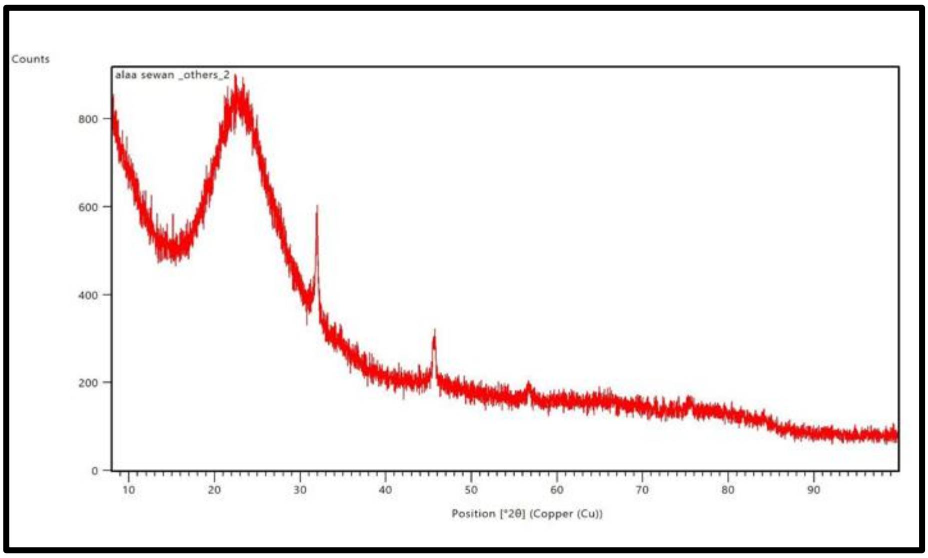

Figure 6. X-ray of nanoscale SIO_2 diagnosis

The TEM Photographs of SiO_2/PAM/PAN

Transmission electron microscope (TEM) images show a marked morphological shift toward a nanofibrous structure, where SiO2 particles act as nucleation centers that catalyze the growth of polyaniline chains in a cross-linked and rod-like manner. Superdispersion of nanoparticles is observed within the polymeric fibers without obvious agglomerations, indicating the presence of strong interfacial interactions linking the mineral phase to the organic phase. This lattice cross-linking contributes to the formation of connected paths for the transfer of electrical charges, which enhances the conductive properties of the hybrid compound, in addition to improving its thermal stability. This porous structure with a high surface area confirms the success of the template polymerization process, making the resulting material an effective candidate for chemical sensing and supercapacitor applications[22, 23].

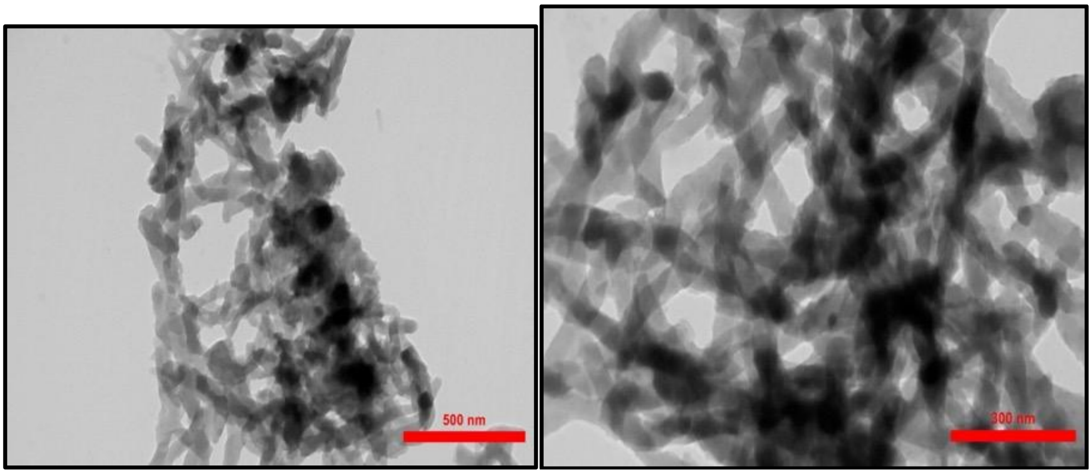

Fig (7): TEM of SiO_2/PAM/PAN

The AFM of Photographs of SiO_2 Nanoparticles

The synthesized silica nanoparticles were analyzed using atomic force microscopy, as shown in Figure (8). The average size of the silica nanoparticles was 81.20 nm. Notably, the two-dimensional and three-dimensional surface dimensions showed no random particle agglomeration, indicating a high degree of homogeneity. Furthermore, the surface area ratio (SDR) was 10.36%, while the average roughness (Sa) was 54.08 and the average square height (Sq) was 67.98. Additionally, the number of elements within the measured area was 369, representing 32.48% of the total surface area[24], as shown in Figure (8).

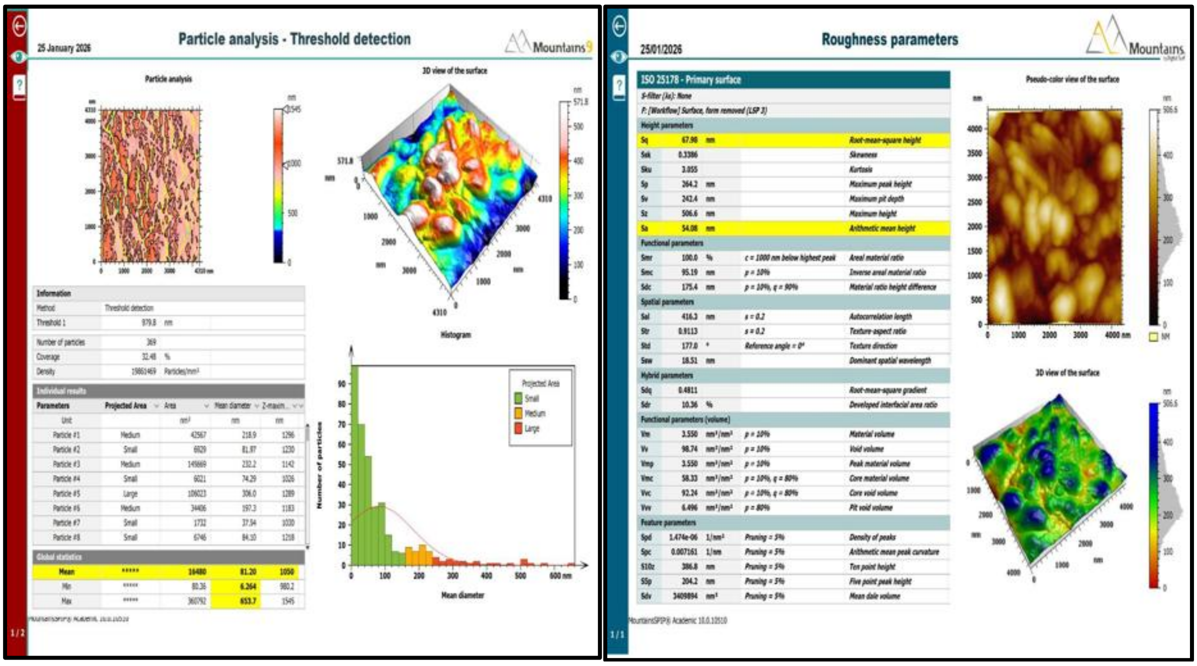

Information		
Method	Threshold detection	
Threshold 1	979.8	nm
Number of particles	369	
Coverage	32.48	%
Density	19861469	Particles/mm²

Individual results

Parameters	Projected Area	Area	Mean diameter	Z-maxim...
Unit		nm²	nm	nm
Particle #1	Medium	42567	218.9	1296
Particle #2	Small	6929	81.97	1230
Particle #3	Medium	149669	232.2	1142
Particle #4	Small	6021	74.29	1026
Particle #5	Large	109023	306.0	1289
Particle #6	Medium	34406	197.3	1183
Particle #7	Small	1732	37.94	1030
Particle #8	Small	6746	84.10	1218

Global statistics

Mean	*****	16480	81.20	1050
Min	*****	80.36	6.264	980.2
Max	*****	360792	653.7	1545

ISO 25178 - Primary surface

S-filter (λs): None

F: [Workflow] Surface, form removed (LSP 3)

Height parameters				
Sq	67.98	nm		Root-mean-square height
Ssk	0.3386			Skewness
Sku	3.055			Kurtosis
Sp	264.2	nm		Maximum peak height
Sv	242.4	nm		Maximum pit depth
Sz	506.6	nm		Maximum height
Sa	54.08	nm		Arithmetic mean height
Functional parameters				
Smr	100.0	%	c = 1000 nm below highest peak	Areal material ratio
Smc	95.19	nm	p = 10%	Inverse areal material ratio
Sdc	175.4	nm	p = 10%, q = 90%	Material ratio height difference
Spatial parameters				
Sal	416.3	nm	s = 0.2	Autocorrelation length
Str	0.9113		s = 0.2	Texture-aspect ratio
Std	177.0	°	Reference angle = 0°	Texture direction
Ssw	18.51	nm		Dominant spatial wavelength
Hybrid parameters				
Sdq	0.4811			Root-mean-square gradient
Sdr	10.36	%		Developed interfacial area ratio
Functional parameters (volume)				
Vm	3.550	nm³/nm²	p = 10%	Material volume
Vv	98.74	nm³/nm²	p = 10%	Void volume
Vmp	3.550	nm³/nm²	p = 10%	Peak material volume
Vmc	58.33	nm³/nm²	p = 10%, q = 80%	Core material volume
Vvc	92.24	nm³/nm²	p = 10%, q = 80%	Core void volume
Vvv	6.496	nm³/nm²	p = 80%	Pit void volume
Feature parameters				
Spd	1.474e-06	1/nm²	Pruning = 5%	Density of peaks
Spc	0.007161	1/nm	Pruning = 5%	Arithmetic mean peak curvature
S10z	386.8	nm	Pruning = 5%	Ten point height
S5p	204.2	nm	Pruning = 5%	Five point peak height
Sdv	3409894	nm³	Pruning = 5%	Mean dale volume

MountainsSPIP® Academic 10.0.10510

Figure 8. AFM of SiO2 Nanoparticles

The SEM of Photographs of SiO2 Nanoparticles

The scanning electron microscope (SEM) is a sophisticated and versatile instrument, widely used to observe the surface characteristics of materials and to provide information about the size and shape of nanoparticles. The SEM image revealed silicon oxide nanoparticles with a size ranging from 43.71 to 77.29 nm[25].

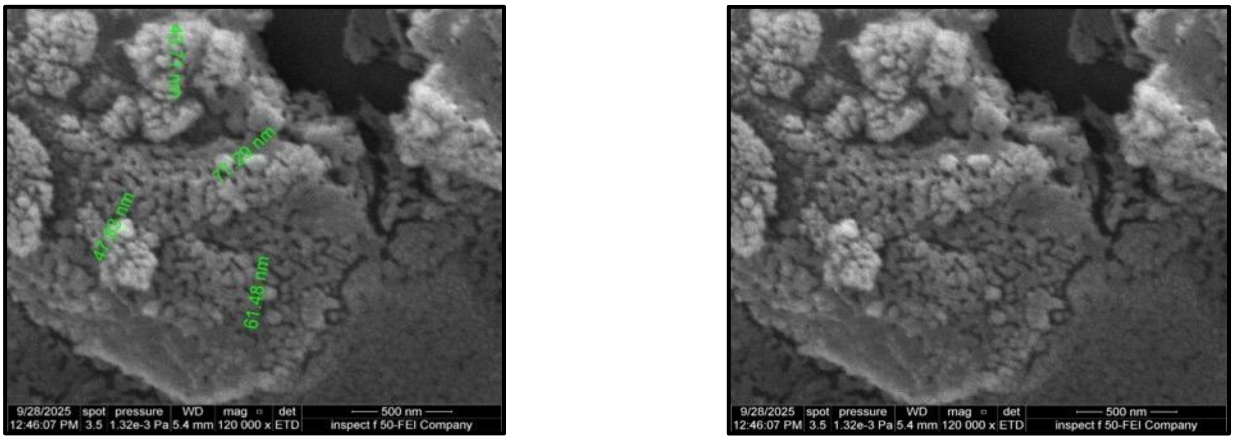

Figure 9. SEM of SiO2 Nanoparticles

Thermogravimetic analysis (TGA) of SiO_2 /PAM/PAN

Figure 3-44 shows the thermogravimetric analysis (TGA), differential thermogravimetric analysis (DTG), and differential scanning calorimetry (DSC) curves for the PAM1 polymer. The TGA curve shows three main phases of weight loss. The first phase occurs at approximately 80 °C and is due to the loss of moisture and volatile substances. The second phase appears at approximately 152 °C and indicates the beginning of partial decomposition of the polymer chains, while the third phase at 227 °C represents the main phase of thermal decomposition of the polymer. The DTG curve confirms these phases by showing distinct peaks at the same temperatures, representing the highest rate of weight loss. The DSC curve shows a thermal signal at lower temperatures attributed to moisture evaporation, as well as other signals at higher temperatures associated with structural changes and the onset of thermal decomposition. Weight loss continues gradually until the end of the experiment at 900 °C, leaving a residual weight of 15.15%. This is attributed to the presence of inorganic SiO_2 molecules with high thermal stability[26, 27].

\

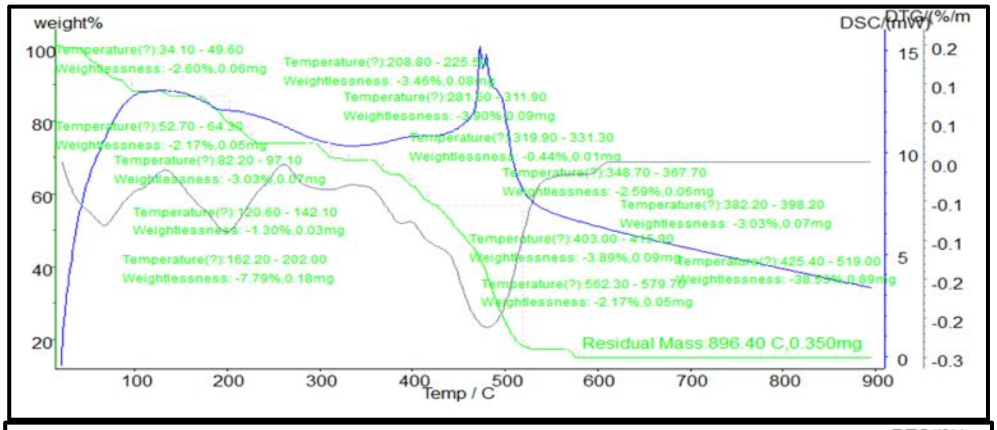

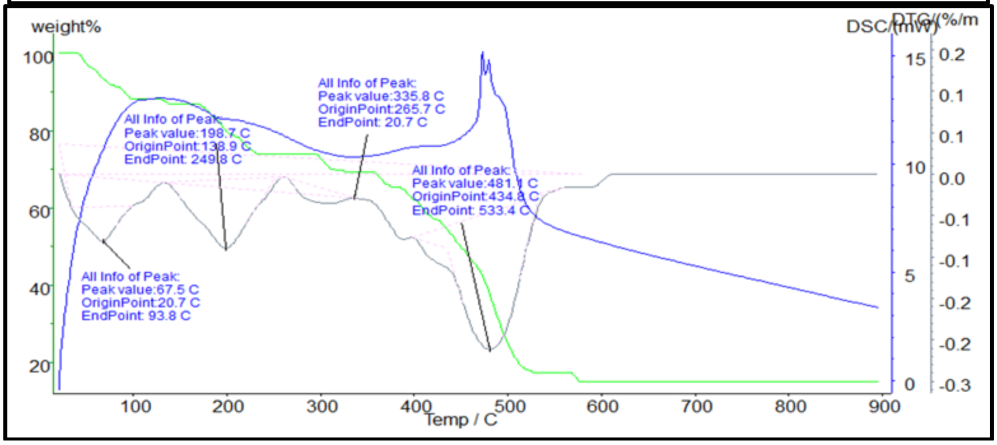

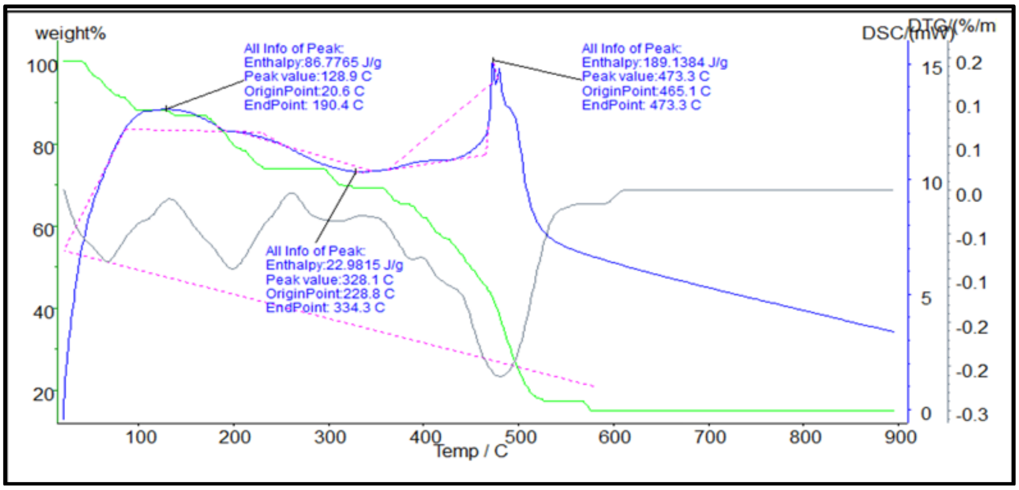

Figure 10. TGA&DSC&DTC of SiO2/PAM/PAN

GPC diagnostic study of SiO2/PAM1/An polymer

The GPC assay results for the prepared polymer, as shown in Table (1), revealed a numerical molecular weight (Mn) of approximately 13,500 g/mol, a gravimetric molecular weight (Mw) of 32,400 g/mol, and a maximum molecular weight (Mz) of 58,900 g/mol. The higher gravimetric molecular weight compared to the numerical molecular weight indicates the presence of polymer chains of varying lengths within the sample. Mw is more affected by longer chains than Mn, suggesting the formation of a polymer with chains of varying lengths as a result of the polymerization reaction. The dispersion index (DPI) of 2.4, greater than 1, indicates a moderately broad molecular weight distribution. Furthermore, the higher Mz value compared to both Mn and Mw confirms the presence of some chains with higher molecular weights. These results generally indicate successful polymerization and the formation of a polymer with a relatively medium to high molecular weight and an acceptable molecular weight distribution. The efficiency of the condensation reaction between monomers and the formation of stable polymer chains can be determined by the preparation conditions used, such as temperature, reaction time, and solvent type. These factors played a role in determining the final molecular weight and its distribution[28, 29].

Table 1. shows the values of the SiO2/PAM/An functions

$SiO_2/PAM_1/An$	Mn g.mol $^{-1}$	Mw g.mol $^{-1}$	Mz g.mol $^{-1}$	D
	13500	32400	58900	2.4

References

1. Li, H., et al., *Recent research progress and advanced applications of silica/polymer nanocomposites.* Nanotechnology Reviews, 2022. **11**(1): p. 2928-2964.
2. Kumari, C., S. Jadoun, and N.K. Jangid, *Recent advancements in polyaniline-based composites for biological applications: a review.* Materials Advances, 2026.
3. Arora, I., et al. *Polyaniline-Based Nanocomposites for Wastewater Treatment*. in *Macromolecular Symposia*. 2025.
4. Sayed, M.M., et al., *Synthesis, physico-chemical characterization, and environmental applications of meso porous crosslinked poly (azomethine-sulfone) s.* Scientific Reports, 2022. **12**(1): p. 12878.
5. Alizadeh, A. and E. Ahmadi, *Polyaniline and MOF5 functionalized mesoporous silica composite as electrode for high performance symmetric supercapacitor.* Scientific Reports, 2025. **15**(1): p. 40233.
6. El-Kamel, R.S. and A.M. Fekry, *Advanced graphene–silica fume/polyaniline–iron nanoparticle composite electrocatalyst for efficient oxygen reduction in alkaline media.* BMC chemistry, 2025. **19**(1): p. 251.

7. Dzulhijjah, W.A., et al., *Synthesis and characterization of nanosilica from rice husk waste Sigupai varieties endemic to Aceh.* Case Studies in Chemical and Environmental Engineering, 2025. **11**: p. 101145.
8. Yuan, S., et al., *A comparative study on rice husk, as agricultural waste, in the production of silica nanoparticles via different methods.* Materials, 2024. **17**(6): p. 1271.
9. Hamidu, I., et al., *Synthesis of silica and silicon from rice husk feedstock: A review.* Heliyon, 2025. **11**(4).
10. Tezel, R.N. and İ. Kaya, *Synthesis and characterization of fluorescent and thermally stable poly (azomethine-ether) s: Optical and morphological properties.* Polymer, 2025. **323**: p. 128169.
11. Ismaili, J., et al., *Synthesis, Characterization, and Investigation of the Properties of a New Promising Poly (Azomethine) Organic Semiconductor Material.* Materials, 2025. **18**(7): p. 1658.
12. Ghillal, Y., et al., *Synthesis, Characterization, and Antimicrobial Evaluation of a Novel Polyazomethine Derived from p-Phenylenediamine and Terephthaldicarboxaldehyde.* 2025.
13. Stejskal, J. and R. Gilbert, *Polyaniline. Preparation of a conducting polymer (IUPAC technical report).* Pure and applied chemistry, 2002. **74**(5): p. 857-867.
14. Semenova, A., et al., *Synthesis and characterization of polyethylenimine–silica nanocomposite microparticles.* Langmuir, 2021. **38**(1): p. 191-202.
15. Sun, Z., et al., *Influence of chemical grafting method on the performance of SiO2 nanocomposite pour point depressant.* Processes, 2023. **11**(4): p. 1159.
16. Shahadat, M., et al., *Recent advances in chitosan-polyaniline based nanocomposites for environmental applications: a review.* Polymer, 2022. **254**: p. 124975.
17. Mahmood, F.S., H.Q. Hussein, and Z.T. Abdulwahhab, *Preparation and characterization of high surface area nanosilica from Iraqi sand via sol-gel technique.* Journal of Petroleum Research and Studies, 2022. **12**(4): p. 104-117.
18. Toskas, G., et al., *Inorganic/organic (SiO2)/PEO hybrid electrospun nanofibers produced from a modified sol and their surface modification possibilities.* ACS Applied Materials & Interfaces, 2011. **3**(9): p. 3673-3681.
19. Ong, H.R., et al., *Investigation on Silane concentration of SiO2 nanoparticle: FTIR analysis.* Chemical Engineering Transactions, 2023. **106**: p. 1345-1350.
20. Shamsuri, A.A., et al., *Fourier transform infrared spectroscopy study of polymer/filler/ionic liquid composites.* Reviews in Analytical Chemistry, 2025. **44**(1): p. 20250084.
21. Saleh, F.T.A., et al., *Synthesis and characteristics of Silica nanoparticles (SiO2NPs) from Bamboo Leaves Ash by precipitation method.* Sana'a University Journal of Applied Sciences and Technology, 2025. **3**(4): p. 949-953.
22. Ahmad, M.N., et al., *Synthesis, characterization, and antibacterial potential of poly (o-anisidine)/BaSO4 nanocomposites with enhanced electrical conductivity.* Processes, 2022. **10**(9): p. 1878.
23. Baeza, G.P., et al., *Multiscale filler structure in simplified industrial nanocomposite silica/SBR systems studied by SAXS and TEM.* Macromolecules, 2013. **46**(1): p. 317-329.
24. Doman, K.M., et al., *Synthesis of silver and copper nanoparticle using Spirulina platensis and evaluation of their anticancer activity.* International Journal of Environmental Health Research, 2024. **34**(2): p. 661-673.
25. Akhtar, K., et al., *Scanning electron microscopy: Principle and applications in nanomaterials characterization*, in *Handbook of materials characterization*. 2018, Springer. p. 113-145.
26. Vara, D., et al., *Sustainable bio-based adsorbents for simultaneous and efficient removal of hazardous dyes from aqueous solutions.* Toxics, 2024. **12**(4): p. 266.
27. Zhang, Y., et al., *Quaternized salicylaldehyde Schiff base side-chain polymer-grafted magnetic Fe3O4 nanoparticles for the removal and detection of Cu2+ ions in water.* Applied Surface Science, 2023. **611**: p. 155632.
28. Montaudo, G., et al., *Molecular Weight Determination and Structural Analysis in Polydisperse Polymers by Hyphenated Gel Permeation Chromatography/Matrix-Assisted Laser Desorption Ionization—Time of Flight Mass Spectrometry.* International Journal of Polymer Analysis and Characterization, 1997. **3**(2): p. 177-192.
29. Ouano, A., *Recent Advances in Gel Permeation Chromatography.* Rubber Chemistry and Technology, 1981. **54**(3): p. 535-575.